THE JOURNAL OF PHYSICAL CHEMISTRY A
A JOURNAL OF THE AMERICAN CHEMICAL SOCIETY

pubs.acs.org/JPCA Article

Millimeter/Submillimeter-wave Spectroscopy and the Semi-experimental Equilibrium (r_e^{SE}) Structure of 1*H*-1,2,4-Triazole (*c*-$C_2H_3N_3$)

Hayley A. Bunn, Brian J. Esselman, Peter R. Franke, Samuel M. Kougias, Robert J. McMahon,* John F. Stanton,* Susanna L. Widicus Weaver,* and R. Claude Woods*

Cite This: *J. Phys. Chem. A* 2022, 126, 8196–8210 Read Online

ACCESS | Metrics & More | Article Recommendations | Supporting Information

Downloaded via UNIV OF WISCONSIN-MADISON on November 16, 2022 at 19:32:24 (UTC).
See https://pubs.acs.org/sharingguidelines for options on how to legitimately share published articles.

ABSTRACT: The millimeter/submillimeter spectrum of 1*H*-1,2,4-triazole is reported from 70 to 700 GHz, providing spectral frequencies directly comparable to radio telescopes and enabling an astronomical search. Using four deuteriated samples of 1,2,4-triazole, we measured, assigned, and least-squares fit transitions for 26 isotopologues to sextic A- and S-reduced Hamiltonians. An accurate and precise semi-experimental (r_e^{SE}) structure from 50 independent moments of inertia has been obtained. Structural parameters are provided with 2σ uncertainties within 0.0009 Å for bond distances and 0.09° for bond angles. The structural parameters are in quite good agreement with the best theoretical estimate (BTE) obtained using CCSD(T)/cc-pCV5Z, where an agreement within the 2σ uncertainty is observed for all but one case. Despite the large number of isotopologues already included in this structure, more may be useful. One isotopologue, [1,3-^{2}H]-1*H*-1,2,4-triazole, is observed to closely approach the oblate asymmetric-top limit, resulting in a clear breakdown of the A-reduction Hamiltonian. The highly accurate r_e^{SE} structure and subsequent analysis demonstrates that the S-reduction is also unable to adequately model the spectrum of this isotopologue.

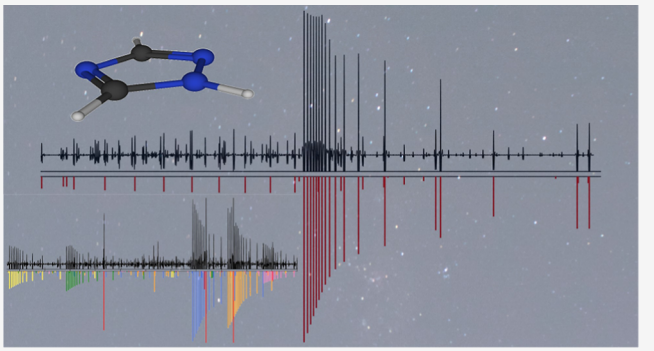

INTRODUCTION

The search for complex organic molecules in the interstellar medium (ISM) and planetary atmospheres is of major importance in understanding the formation and evolution of prebiotic molecules. Among the more than 260 molecules detected in the ISM and circumstellar shells,[1] only 15 of these are cyclic. The recent detection of benzene,[2] benzonitrile,[3,4] 1- and 2-cyanonaphthalene,[5] and 1-cyano-1,3-cyclopentadiene[6] indicates that aromatic nitriles do form even in low-temperature and low-density environments. While there are no confirmed detections of nitrogen-containing heterocycles in the ISM, the tentative detection of the nitrogen-containing three-membered ring aziridine, $(CH_2)_2NH$, reported in 2001 warrants a new search for that molecule, as well as for other nitrogen-containing cyclic compounds.[7] Nitrogen-containing aromatic compounds play a crucial role in terrestrial biochemistry and therefore are important prebiotic targets. To facilitate observational searches for 1,2,4-triazole in Titan's atmosphere or in the ISM, its rotational spectrum was measured in a frequency range that overlaps with that of observational facilities.

The experimental characterization of Titan aerosols by investigation of the formation of tholins by electric discharge resulted in the detection of multiple organic nitrogen-containing species, including 1*H*-1,2,4-triazole.[8] The gas mixture in that study was composed of 95% N_2 and 5% CH_4 to match the atmosphere of Titan. UV photoprocessing of Titan's atmosphere primarily results in HCN and more complex nitrogen-containing species, such as CH_3C_3N, whose detection was recently reported using the ALMA (Atacama Large Millimeter/submillimeter Array) telescope.[9] Ring-containing species, such as 1,2,4-triazole, have been predicted to form from known Titan atmospheric components, beginning with HCN and NH_3.[10−13] Thus, 1*H*-1,2,4-triazole is a prime target for detection in the atmosphere of Titan and other extraterrestrial N- and C-rich environments.

There are two aromatic triazole regioisomers (1,2,3-triazole and 1,2,4-triazole) that differ in their arrangements of the N- and C-atoms of the aromatic ring, Figure 1. Each of these regioisomers exists as an equilibrium mixture of tautomers.

Received: August 23, 2022
Revised: September 22, 2022
Published: October 31, 2022

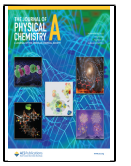

ACS Publications © 2022 American Chemical Society

https://doi.org/10.1021/acs.jpca.2c06038
J. Phys. Chem. A 2022, 126, 8196–8210

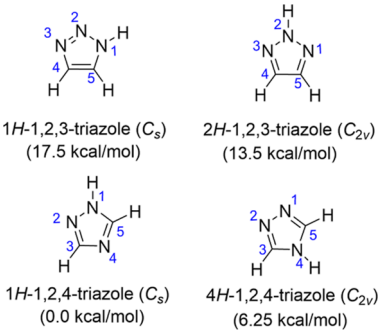

Figure 1. Tautomers of 1,2,3-triazole and 1,2,4-triazole with standard numbering of ring atoms and relative energies at CCSD(T)/CBS.[14]

The tautomers of 1,2,4-triazole, where the N-atoms are separated, are more stable than both the tautomers of 1,2,3-triazole, where all three N-atoms are adjacent. The structure and spectroscopy of 1,2,3-triazole is the subject of a recent study.[15] 1,2,4-Triazole, the subject of this work, exists as 1*H*-1,2,4-triazole (C_s) and 4*H*-1,2,4-triazole (C_{2v}), where the unsymmetrical 1*H*-tautomer is the energetically favored isomer by 6.7 kcal/mol,[16] Figure 1 (bottom). All previous spectroscopic studies have reported detection of only the more stable 1*H*-tautomer. The first gas-phase microwave study of 1,2,4-triazole was reported in 1975 by Bolton *et al.*,[17,18] including analysis of the structure and nuclear quadrupole coupling. Low-resolution gas-phase infrared[19,20] and Raman[20] spectra have been reported between approximately 500 and 4000 cm^{-1} for 1*H*-1,2,4-triazole, providing estimates of the vibrational band origins.

The structure of 1,2,4-triazole has been the focus of multiple studies, involving X-ray crystallography,[21,22] microwave spectroscopy,[17] electron diffraction,[23] and computational methods.[24−26] The rotational constants reported in the gas-phase microwave work were determined for only three isotopologues,[17] which did not provide sufficient information to adequately determine its structural parameters (1*H*-1,2,4-triazole has 13 independent structural parameters, which require a minimum of seven isotopologues to provide a sufficient number of independent moments of inertia for a complete structure determination). The structure was further analyzed by electron diffraction,[23] resulting in additional experimentally determined structural parameters, to a 3σ uncertainty of 0.004−0.01 Å for bond distances and 0.5−1.3° for bond angles. In that work, not all parameters could be satisfactorily determined, so several parameters had to be constrained to computational predictions or values from similar molecules. Semi-experimental (r_e^{SE})[27−32] structures were pioneered in 1978[32] and have recently been applied to various heterocycles.[27−31,33−37] Recent studies on heteroaromatic compounds[38−41] have set a new standard for the determination of accurate and precise semi-experimental equilibrium (r_e^{SE}) structures. The methodology employs well-determined rotational constants for as many isotopologues as is practical, far exceeding the minimal requirement, and CCSD(T) corrections to determine the semi-experimental equilibrium structure. This method results in accurate structural parameters, where the typical 2σ uncertainty is less than 0.0005 Å for bond distances and 0.05° for angles.

In order to more accurately determine the structure of 1*H*-1,2,4-triazole and to provide accurate frequencies to guide observational studies, the millimeter/submillimeter spectrum has been collected from 70 to 700 GHz. The experiment, spectral analysis, and structural determination are presented here. The extension of the spectral range observed in the previous work has allowed for the further refinement of rotational constants for three previously reported isotopologues[17] and spectroscopic constants for an additional 23 isotopologues. A new r_e^{SE} structure has been determined using 50 independent moments of inertia (excluding one isotopologue, *vide infra*) including isotopic substitution of all atoms in multiple isotopologues. Reported transition frequencies and spectroscopic constants can be reliably used to predict the spectrum up to 1 THz and used to guide the search of 1*H*-1,2,4-triazole in Titan's atmosphere and elsewhere in the universe.

EXPERIMENTAL DETAILS

A commercially available sample of 1,2,4-triazole (97%) was used without further purification. 1,2,4-Triazole is a white solid with very low volatility at room temperature compared to other heteroaromatics studied previously.[38−41] Therefore, it was necessary to employ a cell that could be operated at high temperatures. The sample was introduced into a 2 m long stainless-steel cell with a base pressure of 15 mTorr. The cell was equipped with a millimeter/submillimeter spectrometer, described previously.[42] In brief, the spectrometer is composed of a microwave synthesizer (Agilent Technologies, E8257D PSG), Virginia Diodes Inc. frequency multipliers with varying doublers and triplers to cover the frequency region from 70 to 700 GHz, an InSb Hot electron bolometer (QMC Ltd. model QFI/2BI with a closed-cycle He refrigerator), and a lock-in amplifier (Stanford Research Systems SR830 DSP). The cell was heated to a temperature of ∼100 °C, and the spectrum was acquired with a total cell pressure of approximately 30 mTorr at a continuous flow. A single sweep of the spectrum was collected at a step size of 0.1 MHz.

Deuteriation of both the nitrogen and carbon atoms of 1*H*-1,2,4-triazole is remarkably facile compared to other aromatic heterocycles, for example, pyridazine, pyrimidine, or thiazole, due to its amphoteric nature. The pK_{a1} of 1,2,4-triazolium (*N*-protonated 1,2,4-triazole) is 2.45, and the pK_{a2} of 1,2,4-triazole is 10.26.[43] The acidity and basicity of 1*H*-1,2,4-triazole allow easy exchange of the H atoms with D_2O, even at moderate pH values. The exchange at the N atom is most rapid, but exchange at both the C and N atoms can be observed by simple recrystallization of 1,2,4-triazole in D_2O. It is presumed that exchange at the carbon atoms proceeds by an addition−elimination mechanism via a zwitterionic intermediate similar to that described for thiazole.[40,44,45] Taking advantage of the differential rate of exchange between N−H and C−H and the choice of solvent (D_2O or H_2O), four different deuterium-enriched samples were prepared with different species as the predominant isotopologue, as shown in Table 1. This allowed for the observation of all deuteriated 1*H*-1,2,4-triazoles, as well as many of their ^{13}C and ^{15}N isotopologues in natural abundance. The spectral ranges collected for the deuterium-enriched samples were limited to 90 to 335 GHz for sample number 2 and 225 to 335 GHz for the remainder. The details of the synthesis and purification are provided in the Supporting Information. Table 1 provides a numbering scheme and description of the four different deuterium-enriched samples, including the most prominent isotopologues in each sample, their relative abundance determined by comparing multiple

https://doi.org/10.1021/acs.jpca.2c06038
J. Phys. Chem. A 2022, 126, 8196−8210

Table 1. Commercial and Deuteriated Samples of 1*H*-1,2,4-Triazole

sample	preparation[a]	deuterium isotopologues present[b]	relative abundances	frequency range (GHz)
1	none			70−700
2	short deuteriation	**[1-^{2}H]**	1.000	90−335
3	long deuteriation	**[1-^{2}H]**	1.000	225−335
		[3-^{2}H]	0.140	
		[5-^{2}H]	0.252	
		[1,3-^{2}H]	0.275	
		[1,5-^{2}H]	0.325	
		[3,5-^{2}H]	0.473	
		[1,3,5-2H]	0.668	
4	partial protiation (from sample 2)	**[1,5-^{2}H]**	1.000	225−335
		[3-^{2}H]	0.352	
		[5-^{2}H]	0.419	
5	partial protiation (from sample 3)	**[3,5-^{2}H]**	1.000	225−335
		[3-^{2}H]	0.423	
		[5-^{2}H]	0.517	

[a]See the Supporting Information for a full description of the preparation procedures. [b]The isotopologue with the strongest transitions in each sample are in bold.

rotational transitions for each isotopologue, and the frequency range.

COMPUTATIONAL DETAILS

Initial geometry optimization and spectral prediction of the normal isotopologue of each tautomer were performed using the density functional theory [B3LYP/6-311+G(2d,p)] using Gaussian 16.[46] Additional calculations, including geometry optimization, anharmonic second-order vibrational perturbation theory (VPT2), and magnetic property calculations to provide electron-mass corrections were carried out using a developmental version of CFOUR.[47] Coupled-cluster with singles, doubles, and perturbative triples [CCSD(T)] calculations were performed with the cc-pCV*X*Z (*X* = D, T, Q, and 5) basis sets and include the correlation of all electrons. The *xrefit* module of CFOUR was utilized to obtain the least-squares fit r_e^{SE} structure. An iterative approach to the implementation of the structure fitting program, *xrefit*, has been automated in the program *xrefiteration*. The latter program, which is useful in analyzing data sets involving a large number of isotopologues, has been described previously.[39]

SPECTRAL ANALYSIS

Ground-State Spectrum of the Normal Isotopologue of 1*H*-1,2,4-Triazole. The dominant tautomer, 1*H*-1,2,4-triazole, is a near-oblate (κ = 0.824) asymmetric top of C_s symmetry with *a*- and *b*-axis dipole moment components (μ_a = 0.810 ± 0.090 D, and μ_b = 2.579 ± 0.060 D[17]), as shown in Figure 2. The normal isotopologue rotational spectrum in the ground vibrational state was initially predicted using the rotational constants reported from the previous microwave work[17] and the B3LYP quartic and sextic distortion constants. 4*H*-1,2,4-Triazole has C_{2v} symmetry and a strong *a*-type dipole moment (μ_a = 5.77 D, B3LYP). The spectral prediction for the 4*H*-tautomer was performed using B3LYP computed constants and is provided in the Supporting Information. Unsurprisingly,

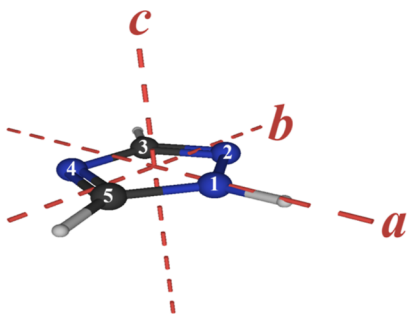

Figure 2. Structure of 1*H*-1,2,4-triazole with principal inertial axes and systematic atom numbering (κ = 0.824, μ_a = 0.810 ± 0.090 D, and μ_b = 2.579 ± 0.060 D).[17]

due to its high relative energy and low equilibrium population, no transitions of 4*H*-1,2,4-triazole were observed in our experimental spectrum. A least-squares fit was performed for the spectrum of 1*H*-1,2,4-triazole to both A- and S-reduced Hamiltonians in the III^l representation, using Pickett's SPFIT/SPCAT program suite[48] and Kisiel's Assignment and Analysis of Broadband Spectra (AABS) software package.[49,50] All experimental spectroscopic constants were converted from the III^l representation to the III^r representation for comparison of theory and experiment. The spectrum of 1*H*-1,2,4-triazole is dominated by typical oblate-type band structures, where transitions increase in K_a, starting from K_a = 0, and decrease in *J* with increasing frequency, as seen in Figure 3. Each observed transition is composed of four components, corresponding to two *a*- and two *b*-type R-branch transitions ($^aR_{0,1}$, $^bR_{1,1}$, and $^bR_{-1,1}$), where the *b*-type components are the most intense. These band structures are observed at regular intervals separated by ∼2*C* with each K_a = 0 band head increasing in *J* with increasing frequency. Q-branch transitions are observed underlying each R-branch band structure, with *J* decreasing with frequency. The transitions in these Q-branch bands are also composed of two *a*-type and two *b*-type components ($^aQ_{2,-1}$, $^aQ_{0,-1}$, and $^bQ_{1,-1}$).

The large number of observed transitions (2514 new and 13 previously reported)[17,18] with the maximum *J* and K_a of almost 100 and 70, respectively (Figure 4), resulted in precise rotational constants and centrifugal distortion parameters up to the sextic level. Table 2 provides these spectroscopic constants for both the A- and S-reductions in comparison to computationally determined CCSD(T)/cc-pCVTZ values. The predicted quartic distortion constants are within 5% of the experimentally determined values, except for δ_J/d_1, which differs by almost 40%, and ϕ_J/h_1 differing by 15.1/11% for the A-/S-reductions. The reasonable agreement of the computed and experimental values validates the use of constants computed at this level in isotopologues where they could not be determined experimentally.

1-*H*-1,2,4-Triazole contains three non-equivalent nitrogen atoms, resulting in very complicated quadrupole coupling interactions. Nuclear quadrupole coupling was introduced into the spectral prediction using the constants presented by Blackman *et al.*[18] Due to the lack of well-resolved hyperfine splitting, however, these parameters could not be improved in this work. Therefore, all spectroscopic parameters presented here were determined without the inclusion of the quadrupole coupling effects into the least-squares fit.

1*H*-1,2,4-Triazole Isotopologues. All singly substituted ^{13}C and ^{15}N isotopologues were observed in natural abundance

https://doi.org/10.1021/acs.jpca.2c06038
J. Phys. Chem. A 2022, 126, 8196−8210

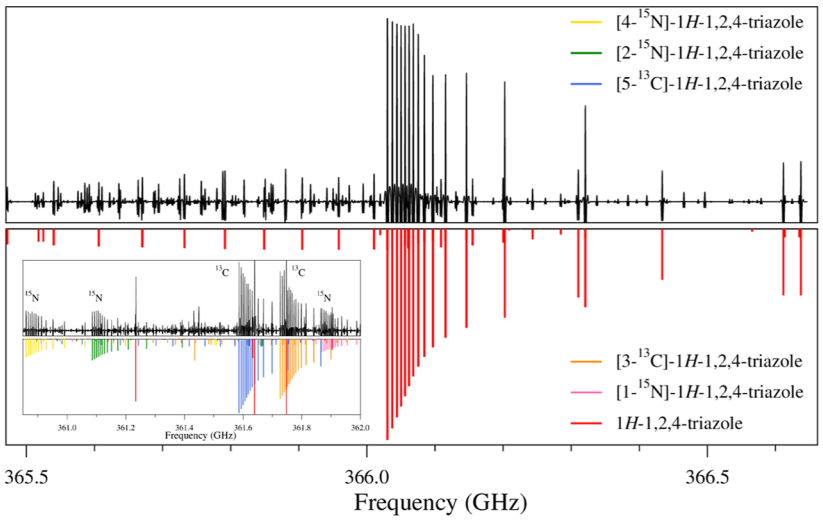

Figure 3. Experimental (top) and predicted (bottom) rotational spectra of the normal isotopologue of 1*H*-1,2,4-triazole from 365.5 to 366.6 GHz. Inset: spectra of ^{13}C and ^{15}N isotopologues from 360.85 to 362.0 GHz observed at natural abundance.

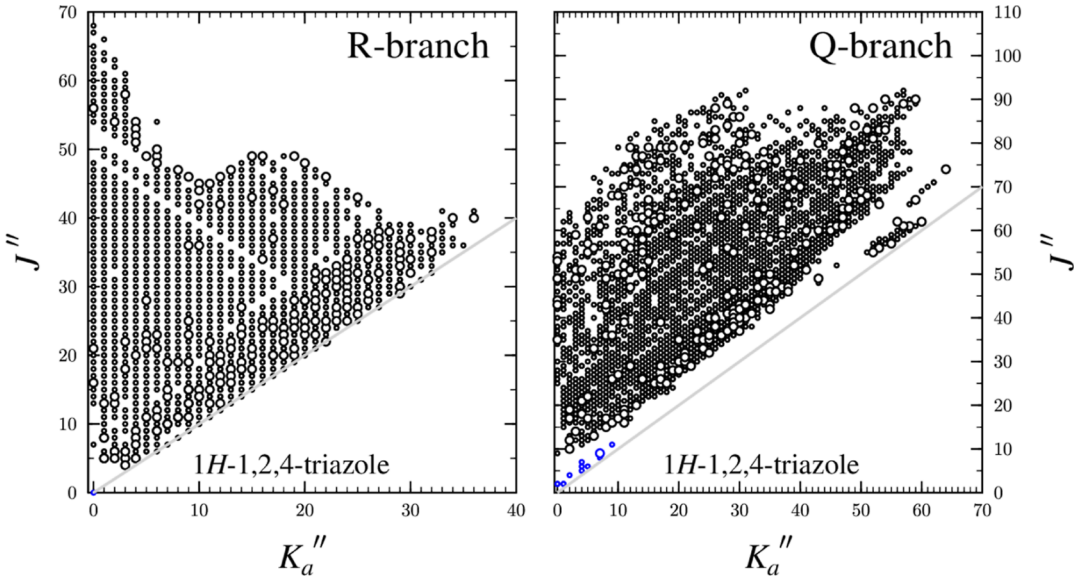

Figure 4. Data distribution plot for 1*H*-1,2,4-triazole from the present work (black) and previous work (blue). The size of the outlined circle is proportional to the value of $|(f_{obs.} - f_{calc.})/\delta f|$, where δf is the frequency measurement uncertainty and all values represented are smaller than 3.

in the spectrum of the commercial sample, as seen in Figure 3. Deuteriated samples were prepared as described above and in the Supporting Information, providing all possible deuteriated combinations. Multiple heavy-atom-substituted deuteriated isotopologues were also observed. Spectra of the singly substituted isopologues were predicted using the isotopic differences in the CCSD(T) spectroscopic constants in combination with the experimental constants of the normal isotopologue. The [3,5-^{2}H]- and [1-^{2}H]-1*H*-1,2,4-triazole isotopologues were predicted using the reported rotational constants in the work by Bolton *et al.*[17] Once a sufficient number of isotopologues were available, an initial r_e^{SE} structure was determined and used to predict the rotational constants of unobserved isotopologues. By combining these constants with the CCSD(T) centrifugal distortion constants, transition frequencies for low K_a series transitions were predicted to within a few megahertz, facilitating searches for additional isotopologues. This was particularly important for finding many of the ^{13}C and ^{15}N isotopologues in the deuteriated samples, where the signal intensities were quite small. Figure 5 shows a segment of the spectrum for sample 4, where multiple isotopologues are observed.

Features similar to those of the normal isotopologue are observed for all other isotopologues. Therefore, the same fitting procedure and parameters were employed for each. The constants were refined to a level of accuracy that is dependent on the number of independent transitions observed, assigned, and included in the least-squares fits. A total of 26 isotolopogues have been observed with enough transitions to determine at least the A_0, B_0, and C_0 rotational constants well. The constants resulting from the S-reduced Hamiltonian in the III^r representation for all singly substituted isotopologues are provided in Table 3. There are obvious similarities between the spectroscopic constants for each isotopologue, and a good agreement is observed between the experimentally and computationally determined constants. Similar to the normal

https://doi.org/10.1021/acs.jpca.2c06038
J. Phys. Chem. A 2022, 126, 8196−8210

Table 2. Spectroscopic Constants for the Ground Vibrational State, Normal Isotopologue of 1*H*-1,2,4-Triazole (A- and S-reduced Hamiltonians, III^r Representation)[a]

	A-reduction			S-reduction	
	CCSD(T)	exp.		CCSD(T)	exp.
$A_0^{(A)}$ (MHz)	10220.8	10245.087700(44)	$A_0^{(S)}$ (MHz)	10220.8	10245.085359(43)
$B_0^{(A)}$ (MHz)	9760.6	9832.076153(40)	$B_0^{(S)}$ (MHz)	9760.6	9832.078475(40)
$C_0^{(A)}$ (MHz)	4990.3	5015.130412(45)	$C_0^{(S)}$ (MHz)	4990.3	5015.130260(45)
Δ_J (kHz)	3.564	3.639025(22)	D_J (kHz)	3.59	3.663059(22)
Δ_{JK} (kHz)	−5.447	−5.582523(24)	D_{JK} (kHz)	−5.601	−5.727076(24)
Δ_K (kHz)	2.278	2.346764(19)	D_K (kHz)	2.407	2.467228(18)
δ_J (kHz)	−0.02926	−0.0433205(91)	d_1 (kHz)	0.02926	0.0433111(90)
δ_K (kHz)	1.118	1.171593(90)	d_2 (kHz)	0.013	0.01204283(92)
Φ_J (Hz)	0.001449	0.0014508(36)	H_J (Hz)	0.001411	0.0014010(35)
Φ_{JK} (Hz)	−0.007308	−0.0073402(38)	H_{JK} (Hz)	−0.006019	−0.0061046(38)
Φ_{KJ} (Hz)	0.01151	0.0115668(46)	H_{KJ} (Hz)	0.00778	0.0079869(45)
Φ_K (Hz)	−0.005655	−0.0056751(34)	H_K (Hz)	−0.003175	−0.0032765(34)
ϕ_J (Hz)	−0.0000672	−0.0000782(16)	h_1 (Hz)	−0.0000703	−0.0000786(16)
ϕ_{JK} (Hz)	−0.0001488	[−0.0001488]	h_2 (Hz)	−0.0000188	[−0.0000188]
ϕ_K (Hz)	0.008973	[0.008973]	h_3 (Hz)	0.0000031	[0.0000031]
N_{lines}[b]		4434	N_{lines}[b]		4434
σ_{fit} (MHz)		0.045	σ_{fit} (MHz)		0.033
κ[c]		0.8421	κ[c]		0.8421
Δ_i (μÅ^2)[d]		0.040904(1)	Δ_i (μÅ^2)[d]		0.040908(1)

[a]Values in square brackets are fixed at the CCSD(T)/cc-pCVTZ value. [b]Number of independent transitions. [c]$\kappa = (2B - A - C)/(A - C)$. [d]$\Delta_i = I_c - I_a - I_b$ calculated using PLANM.

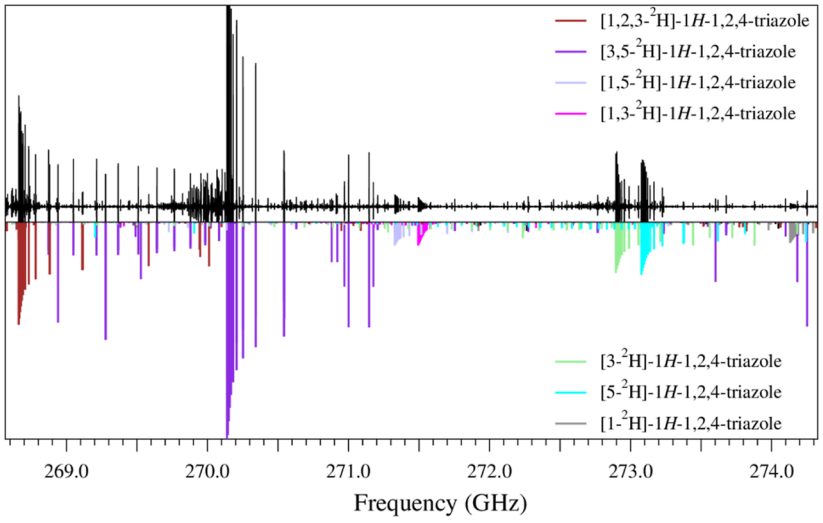

Figure 5. Experimental (top) and predicted (bottom) rotational spectra of deuteriated isotopologues of 1*H*-1,2,4-triazole from 269.6 to 274.3 GHz. Additional transitions due to carbon and nitrogen isotopologues of their deuteriated species are also observed but are not highlighted due to their low intensity in this figure. Transitions in this figure not accounted for in the prediction are likely due to vibrational excited states.

isotopologue, centrifugal distortion constants typically agree within 20%, with the exception of the off-diagonal quartic distortion constants (δ_J/d_1, δ_K/d_2) that vary between 3 and 47%.

Spectroscopic constants from the A-reduced least squares fits of the singly substituted isotopologues and the A- and S-reduced fits for all other isotopologues are presented in the Supporting Information, also showing good agreement with the computed values, with one exception (*vide infra*). The corresponding distribution plots, showing the data set size and breadth of quantum numbers observed for each isotopologue, along with the least-squares fitting output files for each fit are also provided in the Supporting Information. The SPFIT files, including input, output, and line lists for all fits presented here are also available in the Supporting Information. While we observed some transitions that may be assigned for a few additional isotopologues, they were too weak to confidently assign and fit.

When both the A- and S-reductions are adequately treating the data set, the experimental δ_J and $-d_1$ constants will agree with each other to several digits. This relationship can be seen in the spectroscopic constants from any least squares fit or in any set of computed parameters (in this work), except for the fit of [1,3-^{2}H]-1*H*-1,2,4-triazole, as shown in Table 4. This is indicative of the fact that one or both of the reductions are inaccurately determining the constants for this isotopologue. It is clear that the A-reduction, off-diagonal, *K*-dependent terms (δ_K and ϕ_K) were not behaving in a manner similar to that of

https://doi.org/10.1021/acs.jpca.2c06038
J. Phys. Chem. A 2022, 126, 8196−8210

Table 3. Spectroscopic Constants of 1*H*-1,2,4-Triazole Isotopologues (S-reduced Hamiltonian, III^r Representation)[a]

	[3-^{13}C]		[5-^{13}C]		[1-^{15}N]	
	CCSD(T)	exp.	CCSD(T)	exp.	CCSD(T)	Exp.
$A_0^{(S)}$ (MHz)	9979.5	10003.10721(21)	10088.9	10116.58765(14)	10108.3	10136.19906(32)
$B_0^{(S)}$ (MHz)	9759.9	9831.05887(21)	9649.5	9716.44205(13)	9646.4	9713.28028(36)
$C_0^{(S)}$ (MHz)	4931.8	4956.151562(95)	4929.8	4954.227006(85)	4933.5	4958.10645(12)
D_J (kHz)	3.512	3.583925(88)	3.501	3.572293(83)	3.524	3.59552(18)
D_{JK} (kHz)	−5.486	−5.60888(15)	−5.467	−5.58878(14)	−5.495	−5.61791(32)
D_K (kHz)	2.359	2.417594(95)	2.351	2.40942(10)	2.359	2.41778(20)
d_1 (kHz)	0.05141	0.062616(80)	0.05764	0.072897(41)	−0.02565	−0.02304(15)
d_2 (kHz)	0.0042	0.002596(41)	0.026	0.025264(29)	−0.00546	−0.00759(28)
H_J (Hz)	0.001374	0.001337(20)	0.001382	0.001384(19)	0.0001357	0.001273(49)
H_{JK} (Hz)	−0.005847	−0.005955(48)	−0.005854	−0.005922(50)	−0.005815	−0.00598(15)
H_{KJ} (Hz)	0.007554	0.007676(65)	0.007543	0.007718(72)	0.007535	0.00782(21)
H_K (Hz)	−0.003084	−0.003070(38)	−0.003074	−0.003172(36)	−0.003079	−0.003131(99)
h_1 (Hz)	−0.0000239	[−0.0000239]	−0.0000369	[−0.0000369]	−0.0000696	[−0.0000696]
h_2 (Hz)	0.0000847	[0.0000847]	−0.0000726	[−0.0000726]	0.0000707	[0.0000707]
h_3 (Hz)	0.0000038	[0.0000038]	0.0000047	[0.0000047]	0.00002	[0.000002]
N_{line}[b]		1395		1490		892
σ_{fit} (MHz)		0.041		0.037		0.044
κ[c]		0.932		0.845		0.837
Δ_i (μÅ^2)[d]		0.041479(2)		0.041413(2)		0.041319(4)
	[2-^{15}N]		[4-^{15}N]		[1-^{2}H]	
	CCSD(T)	exp.	CCSD(T)	exp.	CCSD(T)	exp.
$A_0^{(S)}$ (MHz)	10194	10219.2185(25)	10209	10233.9235(18)	10014	10055.12879(13)
$B_0^{(S)}$ (MHz)	9528.5	9597.8202(21)	9503.8	9573.2825(14)	9176.6	9226.49583(13)
$C_0^{(S)}$ (MHz)	4922.6	4947.38027(13)	4919.5	4944.28272(11)	4786.5	4809.86098(14)
D_J (kHz)	3.495	3.56722(31)	3.496	3.56771(25)	3.27	3.33610(27)
D_{JK} (kHz)	−5.446	−5.56883(46)	−5.447	−5.56999(37)	−5.081	−5.194262(55)
D_K (kHz)	2.338	2.39597(24)	2.337	2.39570(18)	2.167	2.22170(12)
d_1 (kHz)	0.01294	0.0190(12)	−0.02511	−0.01762(75)	−0.20591	−0.2148130(87)
d_2 (kHz)	0.018	0.0128(13)	−0.0006	−0.00048(97)	−0.025	−0.0235175(33)
H_J (Hz)	0.00135	0.001154(60)	0.001344	0.001175(41)	0.001179	0.00108(16)
H_{JK} (Hz)	−0.005766	−0.00491(23)	−0.005758	−0.00558(14)	−0.005047	−0.005128(11)
H_{KJ} (Hz)	0.007454	0.00643(34)	0.007457	0.00754(22)	0.006555	0.006731(37)
H_K (Hz)	−0.003041	−0.00271(16)	−0.003046	−0.00316(11)	−0.002691	−0.002650(69)
h_1 (Hz)	−0.000061	[−0.000061]	−0.0000662	[−0.0000662]	0.0000206	[0.0000206]
h_2 (Hz)	−0.0000202	[−0.0000202]	0.0000552	[0.0000552]	0.0000403	[0.0000403]
h_3 (Hz)	0.00003	[0.000003]	0.0000007	[0.0000007]	0.0000101	[0.0000101]
N_{line}[b]		787		959		1932
σ_{fit} (MHz)		0.043		0.04		0.032
κ[c]		0.764		0.75		0.684
Δ_i (μÅ^2)[d]		0.041446(17)		0.041539(12)		0.035868(3)
	[3-^{2}H]		[5-^{2}H]		[3,5-^{2}H]	
	CCSD(T)	exp.	CCSD(T)	exp.	CCSD(T)	exp.
$A_0^{(S)}$ (MHz)	9949	9995.23773(28)	9762.9	9834.16097(29)	9637	9700.13103(16)
$B_0^{(S)}$ (MHz)	9152.8	9197.88048(23)	9329.3	9350.76629(28)	8654.2	8679.60003(11)
$C_0^{(S)}$ (MHz)	4764.9	4788.16303(24)	4768.4	4791.33543(19)	4557.6	4579.10318(15)
D_J (kHz)	3.209	3.27477(19)	3.232	3.29914(14)	2.901	2.960923(94)
D_{JK} (kHz)	−5.006	−5.11549(25)	−5.045	−5.15696(20)	−4.51	−4.60813(11)
D_K (kHz)	2.147	2.19835(27)	2.163	2.21421(13)	1.92	1.96496(13)
d_1 (kHz)	−0.08531	−0.08896(20)	−0.2165	-0.23093(19)	−0.2358	−0.248271(68)
d_2 (kHz)	−0.012	−0.01134(21)	0.013	0.01352(17)	−0.01990	−0.020802(44)
H_J (Hz)	0.001294	[0.001294]	0.001261	[0.001261]	0.001142	[0.001142]
H_{JK} (Hz)	−0.005267	−0.005137(81)	−0.005207	−0.005288(54)	−0.004502	−0.004487(29)
H_{KJ} (Hz)	0.00667	0.00655(18)	0.006648	[0.006648]	0.005642	0.005710(76)
H_K (Hz)	−0.002699	[−0.002699]	−0.002705	[−0.002705]	−0.002284	[−0.002284]
h_1 (Hz)	0.0001675	[0.0001675]	0.0001618	[0.0001618]	0.0002534	[0.0002534]
h_2 (Hz)	0.0000139	[0.0000139]	−0.0000234	[−0.0000234]	0.0000603	[0.0000603]
h_3 (Hz)	−0.0000008	[−0.0000008]	−0.0000064	[−0.0000064]	0.0000065	[0.0000065]
N_{line}[b]		491		458		766

https://doi.org/10.1021/acs.jpca.2c06038
J. Phys. Chem. A 2022, 126, 8196−8210

Table 3. continued

	[3-^{2}H]		[5-^{2}H]		[3,5-^{2}H]	
	CCSD(T)	exp.	CCSD(T)	exp.	CCSD(T)	exp.
σ_{fit} (MHz)		0.035		0.033		0.028763
κ[c]		0.694		0.808283		0.6014
Δ_i (μÅ^2)[d]		0.040438(6)		0.040742(5)		0.040077(4)
	[1,5-^{2}H]		[1,3,5-^{2}H]		[1-^{2}H, 3-^{13}C]	
	CCSD(T)	exp.	CCSD(T)	exp.	CCSD(T)	exp.
$A_0^{(S)}$ (MHz)	9659.7	9719.59497(35)	9169.9	9233.86009(23)	9879.1	9925.960(44)
$B_0^{(S)}$ (MHz)	8707.7	8736.00399(25)	8407.7	8427.46382(19)	9083.8	9126.954(39)
$C_0^{(S)}$ (MHz)	4577.7	4599.30603(22)	4384.5	4404.78165(19)	4730.4	4753.22728(48)
D_J (kHz)	2.949	3.00967(15)	2.645	2.69835(12)	3.199	3.2569(38)
D_{JK} (kHz)	−4.575	−4.67588(22)	−4.119	−4.20848(20)	−4.972	−5.0744(86)
D_K (kHz)	1.942	1.98889(14)	1.757	1.79858(31)	2.121	2.1718(50)
d_1 (kHz)	−0.2941	−0.30995(12)	−0.2451	−0.25738(12)	−0.2282	[−0.2282]
d_2 (kHz)	−0.007	−0.00608(13)	−0.005	−0.00629(10)	−0.01549	[−0.01549]
H_J (Hz)	0.001056	[0.001056]	0.0009749	[0.0009749]	0.00115	[0.00115]
H_{JK} (Hz)	−0.004235	−0.004325(48)	−0.003872	−0.004155(43)	−0.00489	[−0.00489]
H_{KJ} (Hz)	0.005574	[0.005574]	0.004867	0.00561(14)	0.00635	[0.00635]
H_K (Hz)	−0.002282	[−0.002282]	−0.001971	−0.00225(16)	−0.00261	[−0.00261]
h_1 (Hz)	0.0001143	[0.0001143]	0.0001811	[0.0001811]	0.0000341	[0.0000341]
h_2 (Hz)	−0.0000169	[−0.0000169]	0.0000158	[0.0000158]	0.0000016	[0.0000016]
h_3 (Hz)	−0.0000007	[−0.0000007]	0.0000029	[0.0000029]	0.0000038	[0.0000038]
N_{line}[b]		399		614		114
σ_{fit} (MHz)		0.036		0.031		0.038
κ[c]		0.6158		0.666		0.6911
Δ_i (μÅ^2)[d]		0.035552(6)		0.035011(5)		0.03632(33)
	[1-^{2}H, 5-^{13}C]		[1-^{2}H, 1-^{15}N]		[1-^{2}H, 2-^{15}N]	
	CCSD(T)	exp.	CCSD(T)	exp.	CCSD(T)	exp.
$A_0^{(S)}$ (MHz)	9776.5	9815.766(10)	10000	10043.662(74)	9839.8	9874.25(12)
$B_0^{(S)}$ (MHz)	9176.2	9226.715(11)	9008.4	9055.122(64)	9098	9153.35(11)
$C_0^{(S)}$ (MHz)	4731.4	4754.44244(43)	4737.2	4760.2868(12)	4725.2	4748.4501(11)
D_J (kHz)	3.189	3.2404(26)	3.219	3.2846(69)	3.185	3.2483(91)
D_{JK} (kHz)	−4.968	−5.0542(57)	−4.989	−5.098(15)	−4.953	−5.065(19)
D_K (kHz)	2.127	2.1684(31)	2.121	2.1712(86)	2.116	2.173(10)
d_1 (kHz)	−0.1605	[−0.1605]	−0.2365	[−0.2365]	−0.1544	[-0.1544]
d_2 (kHz)	−0.02527	[−0.02527]	−0.02825	[−0.02825]	−0.020	[−0.020]
H_J (Hz)	0.001161	[0.001161]	0.001132	[0.001132]	0.00113	[0.00113]
H_{JK} (Hz)	−0.004939	[−0.004939]	−0.004865	[−0.004865]	−0.004861	[−0.004861]
H_{KJ} (Hz)	0.006392	[0.006392]	0.006338	[0.006338]	0.006319	[0.006319]
H_K (Hz)	−0.002617	[−0.002617]	−0.002609	[−0.002609]	−0.002591	[−0.002591]
h_1 (Hz)	0.0000379	[0.0000379]	0.0000211	[0.0000211]	−0.0000059	[−0.0000059]
h_2 (Hz)	0.0000558	[0.0000558]	0.0000468	[0.0000468]	0.0000395	[0.0000395]
h_3 (Hz)	0.0000081	[0.0000081]	0.0000089	[0.0000089]	0.0000081	[0.0000081]
N_{line}[b]		115		49		59
σ_{fit} (MHz)		0.037		0.043		0.048
κ[c]		0.7672		0.6258		0.7187
Δ_i (μÅ^2)[d]		0.036261(84)		0.03607(54)		0.03634(91)
	[1-^{2}H, 4-^{15}N]		[3,5-^{2}H, 3-^{13}C]		[3,5-^{2}H, 5-^{13}C]	
	CCSD(T)	exp.	CCSD(T)	exp.	CCSD(T)	exp.
$A_0^{(S)}$ (MHz)	9990.7	10028.23(11)	9608.2	9672.736(82)	9626.7	9688.46(14)
$B_0^{(S)}$ (MHz)	8949.3	9001.655(99)	8504.4	8527.547(65)	8484.2	8510.11(11)
$C_0^{(S)}$ (MHz)	4718.7	4741.9886(14)	4509.3	4530.4206(11)	4507.7	4528.9155(12)
D_J (kHz)	3.186	3.279(11)	2.848	2.878(11)	2.841	2.9118(98)
D_{JK} (kHz)	−4.937	−5.101(23)	−4.419	−4.459(22)	−4.407	−4.525(21)
D_K (kHz)	2.099	2.176(12)	1.876	1.893(12)	1.87	1.921(11)
d_1 (kHz)	−0.2122	[−0.2122]	−0.2602	[−0.2602]	−0.2445	[−0.2445]
d_2 (kHz)	−0.030	[−0.030]	−0.020	[−0.020]	−0.027	[−0.027]
H_J (Hz)	0.00112	[0.00112]	0.001103	[0.001103]	0.001106	[0.001106]
H_{JK} (Hz)	−0.004811	[−0.004811]	−0.00434	[−0.00434]	−0.004341	[−0.004341]
H_{KJ} (Hz)	0.006264	[0.006264]	0.005444	[0.005444]	0.005438	[0.005438]

https://doi.org/10.1021/acs.jpca.2c06038
J. Phys. Chem. A 2022, 126, 8196−8210

Table 3. continued

	[1-^{2}H, 4-^{15}N]		[3,5-^{2}H, 3-^{13}C]		[3,5-^{2}H, 5-^{13}C]	
	CCSD(T)	exp.	CCSD(T)	exp.	CCSD(T)	exp.
H_K (Hz)	−0.002575	[−0.002575]	−0.002209	[−0.002209]	−0.002204	[−0.002204]
h_1 (Hz)	0.0000107	[0.0000107]	0.0002435	[0.0002435]	0.000243	[0.000243]
h_2 (Hz)	0.0000557	[0.0000557]	0.0000679	[0.0000679]	0.0000733	[0.0000733]
h_3 (Hz)	0.000012	[0.000012]	0.0000066	[0.0000066]	0.000008	[0.000008]
N_{line} [b]		47		62		54
σ_{fit} (MHz)		0.047		0.042		0.038
κ [c]		0.6116		0.554602		0.543235
Δ_i (μÅ^2) [d]		0.03680(83)		0.04026(63)		0.0407(11)
	[3,5-^{2}H, 2-^{15}N]		[1,3,5-^{2}H, 3-^{13}C]		[1,3,5-^{2}H, 5-^{13}C]	
	CCSD(T)	exp.	CCSD(T)	exp.	CCSD(T)	exp.
$A_0^{(S)}$ (MHz)	9515	9574.56(35)	9170.4	9234.476(29)	9103.6	9167.148(44)
$B_0^{(S)}$ (MHz)	8543.8	8571.82(28)	8237.8	8256.767(29)	8295.9	8315.129(40)
$C_0^{(S)}$ (MHz)	4499.6	4521.0873(29)	4337.9	4357.8117(12)	4338.8	4358.8692(11)
D_J (kHz)	2.824	2.887(29)	2.596	2.6631(65)	2.59	2.648(13)
D_{JK} (kHz)	−4.39	−4.479(60)	−4.034	−4.164(14)	−4.033	−4.143(26)
D_K (kHz)	1.871	1.903(30)	1.714	1.7814(72)	1.719	1.779(13)
d_1 (kHz)	−0.1977	[−0.1977]	−0.2630	[−0.2630]	−0.2335	[−0.2335]
d_2 (kHz)	−0.019	[−0.019]	−0.011	[−0.011]	−0.006	[−0.006]
H_J (Hz)	0.001097	[0.001097]	0.000942	[0.000942]	0.0009467	[0.0009467]
H_{JK} (Hz)	−0.00433	[−0.00433]	−0.003729	[−0.003729]	−0.003754	[−0.003754]
H_{KJ} (Hz)	0.005426	[0.005426]	0.00469	[0.00469]	0.004717	[0.004717]
H_K (Hz)	−0.002193	[−0.002193]	−0.001904	[−0.001904]	−0.00191	[−0.00191]
h_1 (Hz)	0.0002403	[0.0002403]	0.0001798	[0.0001798]	0.0001843	[0.0001843]
h_2 (Hz)	0.0000418	[0.0000418]	0.0000314	[0.0000314]	0.000017	[0.000017]
h_3 (Hz)	0.0000033	[0.0000033]	0.0000041	[0.0000041]	0.0000027	[0.0000027]
N_{line} [b]		27		55		43
σ_{fit} (MHz)		0.055		0.042		0.04
κ [c]		0.603148		0.599		0.6456
Δ_i (μÅ^2) [d]		0.0409(27)		0.03555(28)		0.03507(40)
	[1,3,5-^{2}H, 1-^{15}N]		[1,3,5-^{2}H, 2-^{15}N]		[1,3,5-^{2}H, 4-^{15}N]	
	CCSD(T)	exp.	CCSD(T)	exp.	CCSD(T)	exp.
$A_0^{(S)}$ (MHz)	9108.5	9171.50(39)	8980.4	9042.54(89)	8959.7	9022.72(42)
$B_0^{(S)}$ (MHz)	8302.5	8322.66(34)	8374	8394.41(83)	8383.1	8402.85(38)
$C_0^{(S)}$ (MHz)	4341.8	4361.8725(38)	4331.6	4351.9015(52)	4329.3	4349.5435(22)
D_J (kHz)	2.603	2.734(25)	2.574	2.578(46)	2.575	2.657(17)
D_{JK} (kHz)	−4.049	−4.298(50)	−4.016	−3.996(88)	−4.019	−4.187(34)
D_K (kHz)	1.724	1.843(25)	1.718	1.705(41)	1.72	1.809(18)
d_1 (kHz)	−0.2517	[−0.2517]	−0.2012	[−0.2012]	−0.2224	[−0.2224]
d_2 (kHz)	−0.002	[−0.002]	−0.004	[−0.004]	0.000373	[0.000373]
H_J (Hz)	0.0009341	[0.0009341]	0.0009365	[0.0009365]	0.0009327	[0.0009327]
H_{JK} (Hz)	−0.003748	[−0.003748]	−0.003736	[−0.003736]	−0.003735	[−0.003735]
H_{KJ} (Hz)	0.004721	[0.004721]	0.004696	[0.004696]	0.004705	[0.004705]
H_K (Hz)	−0.001914	[−0.001914]	−0.001898	[−0.001898]	−0.001903	[−0.001903]
h_1 (Hz)	0.0001619	[0.0001619]	0.0001905	[0.0001905]	0.0001451	[0.0001451]
h_2 (Hz)	0.0000007	[0.0000007]	0.0000189	[0.0000189]	−0.0000002	[−0.0000002]
h_3 (Hz)	0.0000012	[0.0000012]	0.0000029	[0.0000029]	0.0000017	[0.0000017]
N_{line} [b]		24		18		26
σ_{fit} (MHz)		0.054		0.043		0.04
κ [c]		0.647		0.7236		0.7347
Δ_i (μÅ^2) [d]		0.0364(34)		0.0350(81)		0.0357(38)

[a]Values in square brackets are fixed at the CCSD(T)/cc-pCVTZ value. [b]Number of independent transitions. [c]$\kappa = (2B - A - C)/(A - C)$. [d]$\Delta_i = I_c - I_a - I_b$, calculated using PLANM.

the other isotopologues. When comparing experimentally determined constants of this isotopologue to the other isotopologues in either Hamiltonian reduction, but particularly for the A-reduction, they had large deviations in magnitude and sign. This behavior is a result of the structure of this isotopologue very closely approaching an oblate symmetric top (κ = 0.975). Thus, as has been documented in similar circumstances,[51−56] the A-reduction treatment breaks down when the species approaches a spherical top, a prolate top (in the $I^{r/l}$ representation), or an oblate top (in the $III^{r/l}$

https://doi.org/10.1021/acs.jpca.2c06038
J. Phys. Chem. A 2022, 126, 8196−8210

Table 4. Spectroscopic Constants for the [1,3-^{2}H] Isotopologue of 1*H*-1,2,4-Triazole (A- and S-reduced Hamiltonians, III^r Representation)[a]

	A-reduction			S-reduction	
	CCSD(T)	exp.		CCSD(T)	exp.
$A_0^{(A)}$ (MHz)	9176.5	9236.4108(12)	$A_0^{(S)}$ (MHz)	9176.5	9236.4197(11)
$B_0^{(A)}$ (MHz)	9151.7	9178.1731(11)	$B_0^{(S)}$ (MHz)	9151.7	9178.16473(86)
$C_0^{(A)}$ (MHz)	4580.2	4602.11147(25)	$C_0^{(S)}$ (MHz)	4580.2	4602.11180(22)
Δ_J (kHz)	2.937	2.98908(99)	D_J (kHz)	2.920	2.97925(22)
Δ_{JK} (kHz)	−4.672	−4.7348(55)	D_{JK} (kHz)	−4.571	−4.67224(25)
Δ_K (kHz)	2.052	2.0685(45)	D_K (kHz)	1.968	2.01621(28)
δ_J (kHz)	0.03461	0.0968(34)	d_1 (kHz)	−0.03461	−0.1025(24)
δ_K (kHz)	−14.345	−3.31(28)	d_2 (kHz)	−0.008	−0.00554(42)
Φ_J (Hz)	0.0008944	[0.0008944]	H_J (Hz)	0.001103	[0.001103]
Φ_{JK} (Hz)	0.023781	−0.00834(59)	H_{JK} (Hz)	−0.004544	−0.004552(80)
Φ_{KJ} (Hz)	−0.08551	0.0177(19)	H_{KJ}	0.005777	0.00565(18)
Φ_K (Hz)	0.06083	−0.0106(13)	H_K (Hz)	−0.002337	[−0.002337]
ϕ_J (Hz)	0.001509	[0.]	h_1 (Hz)	0.001513	[0.001513]
ϕ_{JK} (Hz)	0.2569	[0.]	h_2 (Hz)	−0.0001044	[−0.0001044]
ϕ_K (Hz)	−26.8186	[0.]	h_3 (Hz)	−0.0000039	[−0.0000039]
N_{lines}[b]		727	N_{lines}[b]		727
σ_{fit} (MHz)		0.040	σ_{fit} (MHz)		0.040
κ[c]		0.975	κ[c]		0.975
Δ_i (μÅ^2)[d]		0.035505(11)	Δ_i (μÅ^2)[d]		0.035500(10)

[a]Values in square brackets are fixed at the CCSD(T)/cc-pCVTZ value. [b]Number of independent transitions. [c]$\kappa = (2B - A - C)/(A - C)$. [d]$\Delta_i = I_c - I_a - I_b$ calculated using PLANM.

representation). Therefore, we provide the best possible fit for each reduced Hamiltonian, and the predicted values are shown in Table 4, where it is clear that the S-reduction provides a better treatment of the centrifugal distortion. This effect and its use in the structural determination is described in more detail in the discussion below.

Structure Determination. The semi-experimental equilibrium structure (r_e^{SE}) of 1*H*-1,2,4-triazole is determined by using all the moments of inertia from the available isotopologues (excluding [1,3-^{2}H], *vide infra*) with even weighting in the *xrefit* module in CFOUR. Spectroscopic constants determined from both the A- and S-reductions were converted to determinable constants using eqs S.1−S.6 in the Supporting Information. The differences between the A- and S-reduction A_0'', B_0'', and C_0'' determinable constants for all the isotopologues used in the structural determination were very small (<0.006 MHz), providing confidence in both fits. Therefore, the constants used in the r_e^{SE} structure were the average of the determinable constants, corrected for vibration−rotation interactions and electron-mass distributions.

For a rigid, planar molecule, the inertial defect (Δ_{ie}) should be zero. Table 5 shows the inertial defect of 1*H*-1,2,4-triazole, with and without the corrections for vibration−rotation interactions and electron-mass distribution, and it is apparent that the values are approaching zero as these corrections are applied. The behavior of the inertial defect with each correction is similar to that which has been previously observed for the other planar heteroaromatic molecules.[38−41] The uncorrected Δ_{ie} value is around 0.04 μÅ^2. Correction for the vibration−rotation interaction results in a sign reversal and a reduction in the inertial defect to approximately −0.008 μÅ^2, and then, the addition of the electron-mass correction brings the value quite close to zero, with an average value of 0.00102 ± 0.00031 μÅ^2.

The parameters of the r_e^{SE} structure resulting from the final analysis involving 25 isotopologues of 1*H*-1,2,4-triazole are

Table 5. Inertial Defects (Δ_i) of 1*H*-1,2,4-Triazole Isotopologues from Various Determinations of the Moments of Inertia

isotopologue	Δ_{i0} (μÅ^2)	Δ_{ie} (μÅ^2)[a]	Δ_{ie} (μÅ^2)[b]
1*H*-1,2,4-$C_2H_3N_3$	0.04089	−0.00810	0.00108
[3-^{13}C]	0.04150	−0.00804	0.00115
[5-^{13}C]	0.04136	−0.00821	0.00098
[1-^{15}N]	0.04135	−0.00798	0.00121
[2-^{15}N]	0.04143	−0.00811	0.00107
[4-^{15}N]	0.04155	−0.00803	0.00116
[1-^{2}H]	0.03590	−0.00809	0.00110
[3,5-^{2}H]	0.04010	−0.00824	0.00095
[1,3-^{2}H]	0.03569	−0.00799	0.00112
[1,5-^{2}H]	0.03556	−0.00836	0.00083
[1,3,5-^{2}H]	0.03501	−0.00844	0.00075
[1-^{2}H,3-^{13}C]	0.03634	−0.00825	0.00095
[1-^{2}H,5-^{13}C]	0.03631	−0.00819	0.00100
[1-^{2}H,1-^{15}N]	0.03610	−0.00810	0.00110
[1-^{2}H,2-^{15}N]	0.03637	−0.00813	0.00106
[1-^{2}H,4-^{15}N]	0.03683	−0.00772	0.00147
[3-^{2}H]	0.04044	−0.00817	0.00103
[5-^{2}H]	0.04074	−0.00824	0.00095
[1,3,5-^{2}H,3-^{13}C]	0.03555	−0.00831	0.00088
[1,3,5-^{2}H,5-^{13}C]	0.03508	−0.00871	0.00048
[1,3,5-^{2}H,1-^{15}N]	0.03640	−0.00726	0.00193
[1,3,5-^{2}H,2-^{15}N]	0.03503	−0.00885	0.00034
[1,3,5-^{2}H,4-^{15}N]	0.03569	−0.00839	0.00080
[3,5-^{2}H,3-^{13}C]	0.04026	−0.00849	0.00071
[3,5-^{2}H,5-^{13}C]	0.04078	−0.00792	0.00128
[3,5-^{2}H,2-^{15}N]	0.04102	−0.00778	0.00141
average ($\bar{x}$)	0.03820	−0.00816	0.00103
std. dev. (s)	0.00265	0.00031	0.00031

[a]Vibration−rotation interaction corrections only. [b]Vibration−rotation interaction and electron-mass corrections.

https://doi.org/10.1021/acs.jpca.2c06038
J. Phys. Chem. A 2022, 126, 8196−8210

Table 6. Structural Parameters of 1*H*-1,2,4-Triazole

	r_e^{SE}CCSD(T)/cc-pCVTZ	CCSD(T) BTE	CCSD(T)/cc-pCV5Z	CCSD(T)/cc-pCVQZ
R_{C3-H} (Å)	1.0752 (5)	1.0752	1.0751	1.0753
R_{C5-H} (Å)	1.0753 (5)	1.0756	1.0756	1.0757
R_{N1-H} (Å)	1.0031 (5)	1.0031	1.0030	1.0029
R_{C3-N2} (Å)	1.3208 (9)	1.3209	1.3203	1.3209
R_{N1-C5} (Å)	1.3430 (8)	1.3433	1.3426	1.3432
R_{N4-C3} (Å)	1.3605 (8)	1.3616	1.36108	1.3618
R_{N1-N2} (Å)	1.3513 (7)	1.3516	1.35058	1.3513
$\theta_{N2-C3-H}$ (deg)	121.431 (86)	121.480	121.495	121.470
$\theta_{N4-C5-H}$ (deg)	126.566 (89)	126.572	126.581	126.574
$\theta_{N2-N1-H}$ (deg)	120.099 (82)	120.080	120.102	120.091
$\theta_{N1-N2-C3}$ (deg)	101.727 (50)	101.754	101.765	101.712
$\theta_{N2-N1-C5}$ (deg)	110.406 (59)	110.388	110.406	110.419
$\theta_{N2-C3-N4}$ (deg)	115.333 (52)	115.311	115.307	115.377

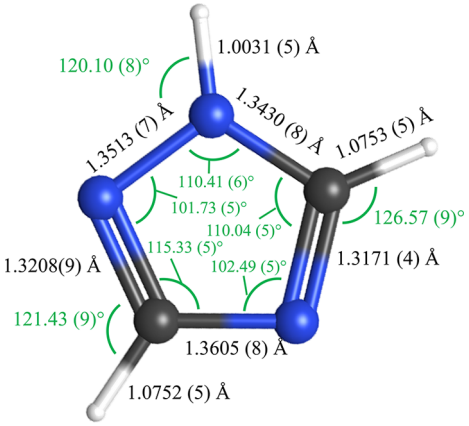

Figure 6. Semi-experimental equilibrium structure (r_e^{SE}) of 1*H*-1,2,4-triazole with 2σ statistical uncertainties from least-squares fitting 25 isotopologue moments of inertia.

presented in Table 6 and depicted in Figure 6. The 2σ statistical uncertainties for the bond distances and bond angles are ≤0.0009 Å and ≤0.09°, respectively. These parameters are determined to a similar accuracy to those of thiazole (0.0009 Å for bond distances and 0.04° for bond angles)[40] and 1*H*-1,2,3-triazole (0.0008 Å for bond distances, 0.006° for internal angles, and 0.2° for external angles)[15] using the same method.

DISCUSSION

Influence of Multiple Isotopic Substitutions on Structure Determination (r_e^{SE}). A commonly used process for determining the structure, Kraitchman analysis,[57] requires the use of all single-substitution isotopologues. While this process is normally sufficient to determine all of the structural parameters of a molecule, it has been shown previously[38−41] that the inclusion of multiply substituted isotopologues can contribute significantly to the accuracy and precision of the structural parameters. Therefore, a structure resulting from more than the singly substituted istopologues is presented here. This analysis provides the opportunity to assess the convergence of the structural parameters, reduce the statistical uncertainty, and determine the accuracy of the computed best theoretical estimate (BTE) structure. Figure 7 shows how the inclusion of each isotopologue beyond the singly substituted data set, which in this case has nine isotopologues, alters the structural parameters, their statistical uncertainties, and their level of agreement with the BTE structure. The *xrefiteration* program starts with this singly substituted data set and then sequentially selects the next isotopologue whose addition results in the minimal statistical uncertainty possible for that number of isotopologues.[39] This provides an analysis of the impact of each of the isotopologues on each of the structural parameters. Examination of the first two angles in the rightmost column of Figure 7 shows how the inclusion of these additional isotopologues beyond the singly substituted dataset is important for converging these parameters. At N_{iso} = 9 for $\theta_{N2-C3-H}$, the magnitude appears reasonable, but the uncertainly of this value is unusually large. The inclusion of just one additional isotopologue results in a significant reduction in the uncertainty. The progression of $\theta_{N4-C5-H}$ shows the importance of including as many isotopologues as is practical as this parameter required the inclusion of at least 22 isotopologues to converge. The examination of R_{N1-N2} required all 25 isotopologues to reach agreement with the BTE. Only one parameter, R_{N4-C3}, is not in 2σ agreement at N_{iso} = 25 with the BTE, where the value exceeds 2σ by 0.0003 Å. As can be seen from the plot in Figure 7, this parameter begins diverging from its corresponding BTE parameter at N_{iso} = 20 and moves further away with the addition of the final isotopologue. This may seem problematic, however; while this parameter diverges, all other parameters either remain in good agreement or move closer to their BTE values when this last isotopologue is incorporated. It is unclear whether additional isotopologues would improve the convergence or agreement with the BTE parameters.

BTE for the Equilibrium Structure of 1*H*-1,2,4-Triazole. The previous section shows an excellent agreement between the semi-experimental equilibrium structure and the BTE for 12 out of 13 parameters. Figure 8 shows the comparison of the r_e^{SE} structure with not only the BTE but also uncorrected structures predicted using CCSD(T) with triple-zeta, quadruple-zeta, and quintuple-zeta basis sets. It is clear that the increase in the basis set provides an increasingly close agreement to the parameters determined for the r_e^{SE} structure. A significant difference is observed between triple-zeta (purple) and quadruple-zeta (gray) basis sets, where the majority of the triple-zeta basis values are outside of the 2σ uncertainty of the r_e^{SE}, while all but one are in agreement for the quadruple-zeta basis. The quintuple-zeta basis set (red) shows a very good agreement in all parameters. In contrast, for all but the one case of R_{N4-C3}, the BTE is in closer agreement to the absolute value and well within the margins of statistical uncertainty. Therefore, the addition of the correction terms

https://doi.org/10.1021/acs.jpca.2c06038
J. Phys. Chem. A 2022, 126, 8196−8210

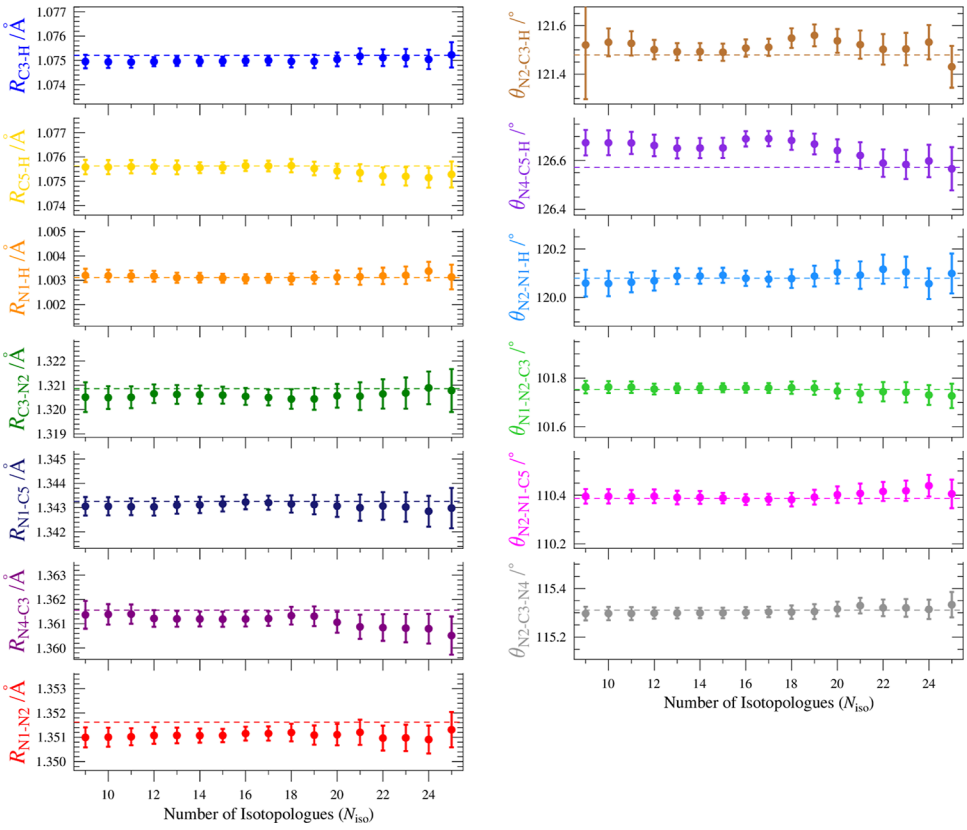

Figure 7. Plots of structural parameters as a function of the number of isotopologues (N_{iso}) and their 2σ uncertainties, with consistent scales for each distance (0.004 Å) and each angle (0.4°). The dashed line in each plot is the BTE value calculated for that parameter.

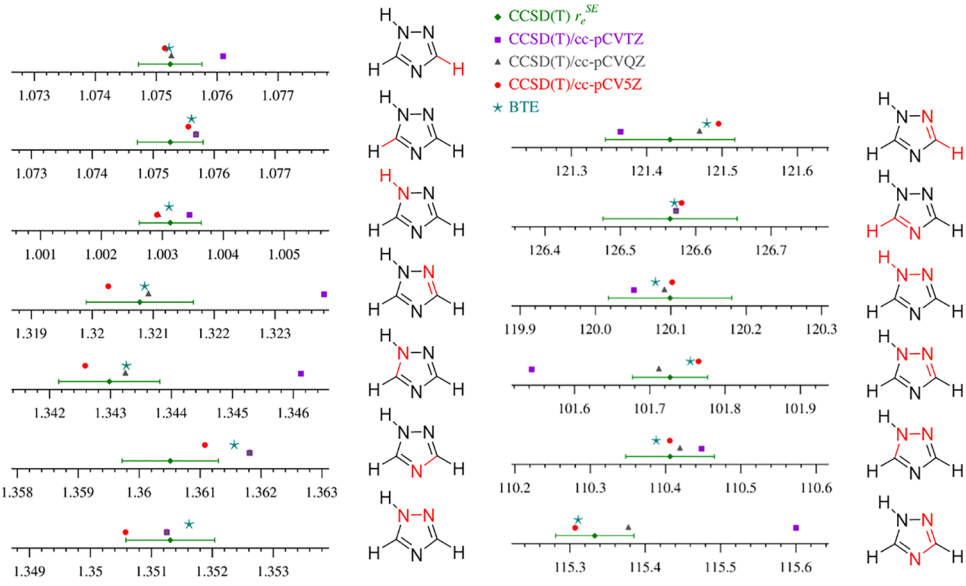

Figure 8. Graphical comparison of the 1*H*-1,2,4-triazole structural parameters with bond distances in angstroms (Å) and angle in degrees (°). The bond lengths are all set to the same scale over 0.0052 Å and angles 0.42°. Uncertainties shown for the r_e^{SE} are 2σ.

including the extrapolation from a quintuple-zeta basis set to an infinite-zeta basis set,[58] estimates of the effects of the inclusion of full triples and perturbative quadruples, inclusion of relativistic effects, and the use of the diagonal Born−Oppenheimer correction (see refs 38−41 for details), shown in Table S7 in the Supporting Information, are expected to provide the best purely theoretical comparison to the r_e^{SE} structure determined here. The corrections for the C−H or N−H distances cause a relatively small change in these parameters between the quintuple-zeta and BTE structures. All of the C−N and N−N bond distances have larger corrections applied to the quintuple-zeta parameters. The parameter in disagreement between the BTE and r_e^{SE} structures (R_{N4-C3}) surprisingly has one of the smaller corrections.

Analysis of the A-reduced Hamiltonian for a Near-Oblate Asymmetric Top. As mentioned earlier, there is

https://doi.org/10.1021/acs.jpca.2c06038
J. Phys. Chem. A 2022, 126, 8196−8210

evidence in the literature showing that the A-reduction is inappropriate for the description of nearly symmetric tops.[54] The asymmetry parameter σ (eq 1) for III^r appears in the most commonly encountered forms of the expressions for the A-reduced quartic centrifugal distortion constants (equations listed in ref 54 and Table 3 of ref 59).

$$\sigma = (2C - A - B)/(A - B) \tag{1}$$

It contains a difference of rotational constants in its denominator and thus may behave analogously to the resonance denominators encountered in the vibrational perturbation theory. When the rotational constants of an asymmetric top approach the prolate symmetric top limit (in the I^r and I^l representations) or the oblate limit (in the III^r and III^l representations), the denominator of σ becomes small, and the value of σ becomes large. Historically, this problem has been solved by changing the representation or reduction.[59]

At the CCSD(T)/cc-pCVTZ level of theory, $\sigma = -21.7$ in the normal triazole isotopologue (which corresponds to $\kappa = +0.824$) versus $\sigma = -369.7$ in the [1,3-^{2}H] isotopologue ($\kappa = +0.989$). The off-diagonal A-reduction constant, δ_K, is unique among the A-reduction quartic constants in that it contains terms that are proportional to σ (eq 3). Thus, it has the capacity to become unreasonably large, leading to a breakdown of the A-reduction. Similarly, all of the K-dependent sextic constants involve terms proportional to σ (see the Supporting Information), but ϕ_K is most sensitive to the breakdown as it contains terms proportional to σ^3 or σ^2 (eq 4).

$$T_N = -T_{xx}^2 + T_{yy}^2 + 2T_{xx}(T_{xy} + T_{xz} - T_{yz}) - 2T_{yy}(T_{xy} - T_{xz} + T_{yz}) - 4T_{xy}(T_{xz} - T_{yz}) \tag{2}$$

$$\delta_K = -\frac{1}{4}(\sigma - 1)T_{xx} - \frac{1}{4}(\sigma + 1)T_{yy} + \frac{1}{2}(\sigma T_{xy}) - \frac{1}{2}(T_{xz} - T_{yz}) \tag{3}$$

$$\begin{aligned}\phi_K = {} & \frac{1}{24}(4\sigma^2 - 3\sigma + 9)\Phi_{xxx} - \frac{1}{24}(4\sigma^2 + 3\sigma + 9)\Phi_{yyy} - \frac{1}{12}(4\sigma^2 - \sigma + 3)\Phi_{xxy} \\ & + \frac{1}{12}(4\sigma^2 + \sigma + 3)\Phi_{yyx} + \frac{1}{6}(\sigma - 3)\Phi_{xxz} + \frac{1}{6}(\sigma + 3)\Phi_{yyz} - \frac{1}{6}\sigma\Phi_{xyz} + \frac{1}{2}(\Phi_{zzx} - \Phi_{zzy}) \\ & + (2B_z - B_x - B_y)^{-1}[-\frac{1}{24}(3\sigma^3 + 2\sigma^2 - 15\sigma)T_{xx}^2 - \frac{1}{24}(3\sigma^3 - 2\sigma^2 - 15\sigma)T_{yy}^2 \\ & + \frac{1}{6}T_{xy}((3\sigma^3 + \sigma^2 - 9\sigma)T_{xx} + (3\sigma^3 - \sigma^2 - 9\sigma)T_{yy}) - \frac{1}{4}(\sigma^3 - 5\sigma)T_{xx}T_{yy} - \frac{1}{2}(\sigma^3 - \sigma)T_{xy}^2 \\ & + \frac{1}{6}(T_{xx} + T_{yy} - 2T_{xy})((\sigma^2 - 6\sigma)T_{xz} - (\sigma^2 + 6\sigma)T_{yz} + 6\sigma T_{zz})]\end{aligned} \tag{4}$$

The breakdown of the A-reduction has also been discussed in relation to the size of the S_{111} parameter from the Watson reduction, that is, the rotational contact transformation, and the relative orders of magnitude of the typical unreduced quartic constant and the difference between the nearly coincident rotational constants.[52,60] Winnewisser first employed the S-reduction in 1972 to fit the extreme near-prolate top, DSSD ($\kappa = -0.999999$).[51] van Eijck proposed the S-reduction independently shortly thereafter.[53] S-reduction eliminates the breakdown problem for nearly symmetric tops. The S-reduced distortion constants appealingly approach those of a true symmetric top in the symmetric top limit. Although the S-reduction constants (except d_1) also contain terms involving σ, they are proportional to $1/\sigma$, which simply goes to zero in the symmetric top limit. The S-reduction was extended to include sextic distortion terms by Typke in 1976.[52] The S-reduction was found to alleviate convergence difficulties and reduce correlations between distortion constants for the nearly oblate tops dimethylsulfoxide ($\kappa = +0.91$) and F_2CO ($\kappa = +0.98$).[52] A similar effect of a very large σ can manifest in the rotational constants. Small centrifugal effects are folded into the rotational constants as a consequence of the rotational contact transformation.[54] These centrifugal corrections also include σ. As with quartic distortion, the A-reduced rotational constants include corrections proportional to σ, while the corrections to the S-reduced rotational constants are proportional to $1/\sigma$. In the limit of large σ (oblate limit), the A-reduced A and B rotational constants receive $\pm$ corrections that are twice the magnitude of the correction to δ_K (eqs 5−7). This effect can be seen in the difference between the fitted A and B rotational constants in the A- and S-reductions. The difference is ∼3× larger in the [1,3-^{2}H] isotopologue (Table 4) than in the normal isotopologue (Table 2). The phenomenon of anomalously large A-reduction corrections to rotational constants was described by Helminger and de Lucia in 1975 for H_2Se, an asymmetric top moderately close to the oblate limit ($\kappa = +0.82$).[61]

$$B_x^{(A)} = B_x - \frac{1}{2}(\sigma + 1)(T_{xx} + T_{yy} - 2T_{xy}) \tag{5}$$

$$B_y^{(A)} = B_y + \frac{1}{2}(\sigma - 1)(T_{xx} + T_{yy} - 2T_{xy}) \tag{6}$$

$$B_z^{(A)} = B_z + T_{xx} + T_{yy} - 2T_{xy} \tag{7}$$

As mentioned above, transitions for a total of 26 isotopologues were assigned and least-squares fit in this work to determine the A_0, B_0, and C_0 constants. In light of the A-reduction breakdown and poor fitting of the [1,3-^{2}H] isotopologue, this isotopologue was excluded, and 25 isotopologues were used to determine the final r_e^{SE} structure of 1H-1,2,4-triazole. Figure S1 of the Supporting Information is the same as Figure 7 but includes this additional isotopologue, $N_{iso} = 26$. Following the inclusion of the [1,3-^{2}H] isotopologue, the parameters appear to drastically increase in statistical uncertainty, and the majority wander further away from the BTE. As mentioned above, the near-oblate symmetric nature of the [1,3-^{2}H] isotopologue results in a breakdown of the A-reduction. Therefore, to prevent any impact of the A-reduction on the structure, only the S-reduction determinable constants were used for this isotopologue. It appears, however, from the inclusion of this isotopologue into the structure that even the S-reduction was not adequate for fitting this isotopologue in the context of structure determination and did not provide A_0'', B_0'', and C_0'' constants sufficiently free of centrifugal distortion. Comparison of the computed and

https://doi.org/10.1021/acs.jpca.2c06038
J. Phys. Chem. A 2022, 126, 8196−8210

experimentally determined distortion constants in Table 4 does not reveal any significant discrepancies. This issue displayed in the [1,3-^{2}H] isotopologue is only noticeable from the analysis of its contribution to the r_e^{SE} structural parameters. Evidence of the breakdown has not been reported previously due to the subtlety of this breakdown, which becomes clear only in the very detailed, high-precision analysis performed in the course of this work.

CONCLUSIONS

The rotational spectrum for 1*H*-1,2,4-triazole from 70 to 700 GHz has been analyzed, and precise rotational and centrifugal distortion constants have been determined. These constants and measured frequencies provide the foundation for the search of 1*H*-1,2,4-triazole in Titan using data from the ALMA radio telescope, which is currently underway.

The 50 independent moments of inertia and breadth of spectroscopic analysis result in highly precise r_e^{SE} structural parameters. The 2σ uncertainties in the determined parameters are comparable in magnitude to previous studies that used the same structural determination methodology.[38−41] In this case, the discrepancy in the N4−C3 distance is an indicator that the inclusion of as many as 25 isotopologues may not be sufficient to determine all 13 structural parameters to the expected accuracy and precision or that some of the constants used are not adequately determined due to the low number of observed transitions. It is noteworthy that neither N4 nor C3 lie close to a principal axis; therefore, their atom positions should be well-determined.

The fit of the [1,3-^{2}H] isotopologue, nearly an oblate symmetric top, resulted in an obvious breakdown of the A-reduction Hamiltonian. While the S-reduction Hamiltonian appeared to treat the transitions for this isotopologue well when comparing the experimentally determined distortion constants to the computed terms, the inclusion of this isotopologue caused an apparent distortion of the structural parameters and a significant increase in the parameter uncertainties. The cause of this effect is not entirely clear and it may be that the inclusion of even more isotopologues would bring this into agreement. An advantage of the precise r_e^{SE} structure is that each isotopologue receives a consistency check from the other 25 isotopologues to provide external validation of the accuracy of the least-squares fit constants. Therefore, the use and analysis of the *xrefiteration* procedure identified a potential problem with the ability to fit a near-oblate symmetric top using the S-reduction method, a problem that would have otherwise gone unnoticed.

ASSOCIATED CONTENT

Supporting Information

The Supporting Information is available free of charge at https://pubs.acs.org/doi/10.1021/acs.jpca.2c06038.

Prediction for 4*H*-1,2,4-triazole (ZIP).

Least-squares fitting for all isotopologues (ZIP)

Magnetic calculations for all 1-*H*-1,2,4-triazole isotopologues, geometry optimization of 1-*H*-1,2,4-triazole, and VPT2 anharmonic output for all 1-*H*-1,2,4-triazole isotopologues (ZIP)

Structure files (ZIP)

In-depth description and supporting analysis of the deuteriation of 1,2,4-triazole, data distribution plots and A-reduced constants for all isotopologues, determinable constants and the equations used to calculate them, and the computational correction used to determine the BTE (PDF)

AUTHOR INFORMATION

Corresponding Authors

Robert J. McMahon − *Department of Chemistry, University of Wisconsin-Madison, Madison, Wisconsin 53706, United States;* orcid.org/0000-0003-1377-5107; Email: robert.mcmahon@wisc.edu

John F. Stanton − *Quantum Theory Project, Departments of Physics and Chemistry, University of Florida, Gainesville, Florida 32611-7200, United States;* orcid.org/0000-0003-2345-9781; Email: johnstanton@chem.ufl.edu

Susanna L. Widicus Weaver − *Department of Chemistry, University of Wisconsin-Madison, Madison, Wisconsin 53706, United States;* orcid.org/0000-0001-6015-3429; Email: slww@chem.wisc.edu

R. Claude Woods − *Department of Chemistry, University of Wisconsin-Madison, Madison, Wisconsin 53706, United States;* orcid.org/0000-0003-0865-4693; Email: rcwoods@wisc.edu

Authors

Hayley A. Bunn − *Department of Chemistry, University of Wisconsin-Madison, Madison, Wisconsin 53706, United States;* orcid.org/0000-0002-7783-3049

Brian J. Esselman − *Department of Chemistry, University of Wisconsin-Madison, Madison, Wisconsin 53706, United States;* orcid.org/0000-0002-9385-8078

Peter R. Franke − *Department of Chemistry, University of Florida, Gainesville, Florida 32611-7200, United States;* orcid.org/0000-0001-9781-3179

Samuel M. Kougias − *Department of Chemistry, University of Wisconsin-Madison, Madison, Wisconsin 53706, United States;* orcid.org/0000-0002-9877-0817

Complete contact information is available at: https://pubs.acs.org/10.1021/acs.jpca.2c06038

Notes

The authors declare no competing financial interest.

ACKNOWLEDGMENTS

We gratefully acknowledge the funding from the National Science Foundation (R.J.M. CHE-1954270), the U.S. Department of Energy, Office of Basic Energy Sciences (J.F.S. DE-SC0018164), and S.L.W.W.'s UW-Madison start-up fund. We thank the following organizations and individuals for the support of shared departmental facilities: Bruker AVANCE 400 NMR spectrometer (NSF CHE-1048642), Bruker AVANCE 500 NMR spectrometer (gift from Paul J. and Margaret M. Bender), and Thermo Scientific Q Exactive Plus mass spectrometer (NIH 1S10 OD020022-1). The authors acknowledge Maria Zdanovskaia for discussions regarding triazole and assistance with figure generation.

REFERENCES

(1) Endres, C. P.; Schlemmer, S.; Schilke, P.; Stutzki, J.; Müller, H. S. The Cologne Database for Molecular Spectroscopy, CDMS, in the Virtual Atomic and Molecular Data Centre, VAMDC. *J. Mol. Spectrosc.* **2016**, *327*, 95−104.

(2) Cernicharo, J.; Heras, A. M.; Tielens, A. G. G. M.; Pardo, J. R.; Herpin, F.; Guélin, M.; Waters, L. B. F. M. *Infrared Space*

Observatory's Discovery of C_4H_2, C_6H_2, and Benzene in CRL 618. *Astrophys. J.* **2001**, *546*, L123−L126.
(3) McGuire, B. A.; Burkhardt, A. M.; Kalenskii, S.; Shingledecker, C. N.; Remijan, A. J.; Herbst, E.; McCarthy, M. C. Detection of the aromatic molecule benzonitrile (c-C_6H_5CN) in the interstellar medium. *Science* **2018**, *359*, 202−205.
(4) Burkhardt, A.; Loomis, R.; Shingledecker, C.; Lee, K. L.; Remijan, A. J.; McCarthy, M. C.; McGuire, B. A. Ubiquitous aromatic carbon chemistry at the earliest stages of star formation. *Nat. Astron.* **2021**, *5*, 181−187.
(5) McGuire, B. A.; Loomis, R. A.; Burkhardt, A. M.; Lee, K. L. K.; Shingledecker, C. N.; Charnley, S. B.; Cooke, I. R.; Cordiner, M. A.; Herbst, E.; Kalenskii, S.; et al. Detection of two interstellar polycyclic aromatic hydrocarbons via spectral matched filtering. *Science* **2021**, *371*, 1265−1269.
(6) McCarthy, M. C.; Lee, K. L. K.; Loomis, R. A.; Burkhardt, A. M.; Shingledecker, C. N.; Charnley, S. B.; Cordiner, M. A.; Herbst, E.; Kalenskii, S.; Willis, E. R.; et al. Interstellar detection of the highly polar five-membered ring cyanocyclopentadiene. *Nat. Astron.* **2021**, *5*, 176−180.
(7) Dickens, J.; Irvine, W.; Nummelin, A.; Møllendal, H.; Saito, S.; Thorwirth, S.; Hjalmarson; Ohishi, M. Searches for new interstellar molecules, including a tentative detection of aziridine and a possible detection of propenal. *Spectrochim. Acta, Part A* **2001**, *57*, 643−660.
(8) He, C.; Smith, M. A. Identification of nitrogenous organic species in Titan aerosols analogs: Nitrogen fixation routes in early atmospheres. *Icarus* **2013**, *226*, 33−40.
(9) Thelen, A. E.; Cordiner, M. A.; Nixon, C. A.; Vuitton, V.; Kisiel, Z.; Charnley, S. B.; Palmer, M. Y.; Teanby, N. A.; Irwin, P. G. J. Detection of CH_3C_3N in Titan's Atmosphere. *Astrophys. J.* **2020**, *903*, L22.
(10) Teanby, N.; Irwin, P.; Dekok, R.; Nixon, C.; Coustenis, A.; Bezard, B.; Calcutt, S.; Bowles, N.; Flasar, F.; Fletcher, L.; et al. Latitudinal variations of HCN, HC_3N, and C_2N_2 in Titan's stratosphere derived from Cassini CIRS data. *Icarus* **2006**, *181*, 243−255.
(11) Teanby, N.; Irwin, P.; de Kok, R.; Vinatier, S.; Bézard, B.; Nixon, C.; Flasar, F.; Calcutt, S.; Bowles, N.; Fletcher, L.; et al. Vertical profiles of HCN, HC_3N, and C_2H_2 in Titan's atmosphere derived from Cassini/CIRS data. *Icarus* **2007**, *186*, 364−384.
(12) Vuitton, V.; Yelle, R.; Anicich, V. The Nitrogen Chemistry of Titan's Upper Atmosphere Revealed. *Astrophys. J.* **2006**, *647*, L175−L178.
(13) Cui, J.; Yelle, R.; Vuitton, V.; Waite, J.; Kasprzak, W.; Gell, D.; Niemann, H.; Müller-Wodarg, I.; Borggren, N.; Fletcher, G.; et al. Analysis of Titan's neutral upper atmosphere from Cassini Ion Neutral Mass Spectrometer measurements. *Icarus* **2009**, *200*, 581−615.
(14) Balabin, R. M. Tautomeric equilibrium and hydrogen shifts in tetrazole and triazoles: Focal-point analysis and ab initio limit. *J. Chem. Phys.* **2009**, *131*, 154307.
(15) Zdanovskaia, M. A.; Esselman, B. J.; Kougias, S. M.; Amberger, B. K.; Stanton, J. F.; Woods, R. C.; McMahon, R. J. Precise equilibrium structures of 1*H*- and 2*H*-1,2,3-triazoles ($C_2H_3N_3$) by millimeter-wave spectroscopy. *Chem. Phys.* **2022**, *157*, 084305.
(16) Lu, Y.-L.; Gong, X.-D.; Ju, X.-H.; Ji, G.-F.; Xiao, H.-M. Structures and Properties of 1,2,3-Triazoles and 1,2,4-Triazoles. *Chin. J. Struct. Chem.* **2006**, *25*, 582−588.
(17) Bolton, K.; Brown, R.; Burden, F.; Mishra, A. The microwave spectrum and structure of 1,2,4-triazole. *J. Mol. Spectrosc.* **1975**, *27*, 261−266.
(18) Blackman, G.; Brown, R.; Burden, F.; Mishra, A. Quadrupole hyperfine structure of the microwave spectrum of 1,2,4-triazole and N-deuterotriazole. *J. Mol. Spectrosc.* **1975**, *57*, 294−300.
(19) Bougeard, D.; Le Calvé, N.; Roch, B. S.; Novak, A. 1,2,4-Triazole: Vibrational spectra, normal coordinate calculations, and hydrogen bonding. *Chem. Phys.* **1976**, *64*, 5152−5164.
(20) Billes, F.; Endrédi, H.; Keresztury, G. Vibrational spectroscopy of triazoles and tetrazole. *J. Mol. Struct.: THEOCHEM* **2000**, *530*, 183−200.
(21) Deuschl, H. Die Röntgen struktur analyse von 1, 2, 4-Triazol. *Ber. Bunsenges. Phys. Chem.* **1965**, *69*, 550−557.
(22) Goldstein, P.; Ladell, J.; Abowitz, G. Refinement of the crystal and molecular structure of 1,2,4-triazole ($C_2H_3N_3$) at low temperature. *Acta Crystallogr., Sect. B: Struct. Crystallogr. Cryst. Chem.* **1969**, *25*, 135−143.
(23) Chiang, J. F.; Lu, K. Molecular structure of 1,2,4-triazole. *J. Mol. Struct.* **1977**, *41*, 223−229.
(24) Cox, J. R.; Woodcock, S.; Hillier, I. H.; Vincent, M. A. Tautomerism of 1,2,3- and 1,2,4-Triazole In the Gas Phase and In Aqueous Solution: A Combined ab Initio Quantum Mechanics and Free Energy Perturbation Study. *J. Phys. Chem.* **1990**, *94*, 5499−5501.
(25) Aziz, S.; Elroby, S.; Alyoubi, A.; Osman, I. O.; Hilal, R. Experimental and theoretical assignment of the vibrational spectra of triazoles and benzotriazoles. Identification of IR marker bands and electric response properties. *J. Mol. Model.* **2014**, *20*, 2078.
(26) Abdulov, K.; Mulloev, N.; Tabarov, S.; Khodiev, M. K. Quantum Chemical Determination of the Molecular Structure of 1,2,4-Triazole and the Calculation of its Infrared Spectrum. *J. Struct. Chem.* **2020**, *61*, 510−514.
(27) Demaison, J. Experimental, semi-experimental and *ab initio* equilibrium structures. *Mol. Phys.* **2007**, *105*, 3109−3138.
(28) Liévin, J.; Demaison, J.; Herman, M.; Fayt, A.; Puzzarini, C. Comparison of the experimental, semi-experimental and *ab initio* equilibrium structures of acetylene: Influence of relativisitic effects and of the diagonal Born-Oppenheimer corrections. *Chem. Phys.* **2011**, *134*, 064119.
(29) Vázquez, J.; Stanton, J. F.*Equilibrium Molecular Structures: From Spectroscopy to Quantum Chemistry*; Demaison, J., et al, Eds.; Taylor Francis, 2010; Chapter 3, pp 53−87.
(30) Mendolicchio, M.; Penocchio, E.; Licari, D.; Tasinato, N.; Barone, V. Development and Implementation of Advanced Fitting Methods for the Calculation of Accurate Molecular Structures. *J. Chem. Theory Comput.* **2017**, *13*, 3060−3075.
(31) Puzzarini, C.; Barone, V. Diving for Accurate Structures in the Ocean of Molecular Systems with the Help of Spectroscopy and Quantum Chemistry. *Acc. Chem. Res.* **2018**, *51*, 548−556.
(32) Pulay, P.; Meyer, W.; Boggs, J. E. Cubic force constants and equilibrium geometry of methane from Hartree-Fock and correlated wavefunctions. *Chem. Phys.* **1978**, *68*, 5077−5085.
(33) Penocchio, E.; Piccardo, M.; Barone, V. Semiexperimental Equilibrium Structures for Building Blocks of Organic and Biological Molecules: The B2PLYP Route. *J. Chem. Theory Comput.* **2015**, *11*, 4689−4707.
(34) Piccardo, M.; Penocchio, E.; Puzzarini, C.; Biczysko, M.; Barone, V. Semi-Experimental Equilibrium Structure Determinations by Employing B3LYP/SNSD Anharmonic Force Fields: Validation and Application to Semirigid Organic Molecules. *J. Phys. Chem. A* **2015**, *119*, 2058−2082.
(35) Penocchio, E.; Mendolicchio, M.; Tasinato, N.; Barone, V. Structural features of the carbon-sulfur chemical bond: a semi-experimental perspective. *Can. J. Chem.* **2016**, *94*, 1065−1076.
(36) Puzzarini, C. Accurate molecular structures of small- and medium-sized molecules. *Int. J. Quantum Chem.* **2016**, *116*, 1513−1519.
(37) Piccardo, M.; Penocchio, E.; Puzzarini, C.; Biczysko, M.; Barone, V. Correction to Semi-Experimental Equilibrium Structure Determinations by Employing B3LYP/SNSD Anharmonic Force Fields: Validation and Application to Semirigid Organic Molecules. *J. Phys. Chem. A* **2016**, *120*, 3754.
(38) Heim, Z. N.; Amberger, B. K.; Esselman, B. J.; Stanton, J. F.; Woods, R. C.; McMahon, R. J. Molecular structure determination: Equilibrium structure of pyrimidine (m-$C_4H_4N_2$) from rotational spectroscopy (r_e^{SE}) and high-level ab initio calculation (r_e) agree within the uncertainty of experimental measurement. *Chem. Phys.* **2020**, *152*, 104303.

https://doi.org/10.1021/acs.jpca.2c06038
J. Phys. Chem. A 2022, 126, 8196−8210

(39) Owen, A. N.; Zdanovskaia, M. A.; Esselman, B. J.; Stanton, J. F.; Woods, R. C.; McMahon, R. J. Semi-Experimental Equilibrium (r_e^{SE})) and Theoretical Structures of Pyridazine (o-$C_4H_4N_2$). *J. Phys. Chem. A* **2021**, *125*, 7976.
(40) Esselman, B. J.; Zdanovskaia, M. A.; Owen, A. N.; Stanton, J. F.; Woods, R. C.; McMahon, R. J. Precise equilibrium structure of thiazole (c-C_3H_3NS) from twenty-four isotopologues. *Chem. Phys.* **2021**, *155*, 054302.
(41) Orr, V. L.; Ichikawa, Y.; Patel, A. R.; Kougias, S. M.; Kobayashi, K.; Stanton, J. F.; Esselman, B. J.; Woods, R. C.; McMahon, R. J. Precise equilibrium structure determination of thiophene (c-C_4H_4S) by rotational spectroscopy-Structure of a five-membered heterocycle containing a third-row atom. *Chem. Phys.* **2021**, *154*, 244310.
(42) Wright, C. J.; Smith, R. N.; Kroll, J. A.; Shipman, S. T.; Widicus Weaver, S. L. Extending the Millimeter/Submillimeter Wave Spectrum of Ground State Pyruvic Acid for Comparison to Astronomical Data. *ACS Earth Space Chem.* **2022**, *6*, 482−495.
(43) Garrett, P. J.*Comprehensive Heterocyclic Chemistry II: a Review of the Literature 1982−1995: the Structure, Reactions, Synthesis, and Uses of Heterocyclic Compounds*; Fagerberg, J., Mowery, D. C., Nelson, R. R., Eds.; Pergamon: Oxford; New York, 1996; Chapter 4.02, pp 127−163.
(44) Coburn, R.; Landesberg, J.; Kemp, D.; Olofson, R. An addition-elimination mechanism for C—H/C—D exchange in thiazole. *Tetrahedron* **1970**, *26*, 685−692.
(45) Belen'kii, L. I.; Nesterov, I.; Chuvylkin, N. Quantum chemical studies of azoles 13. Specific solvation effect on the calculated energetic parameters of the electrophilic substitution mechanism in thiazole via elimination−addition schemes. *Russ. Chem. Bull.* **2018**, *67*, 1971−1977.
(46) Frisch, M. J.; Trucks, G. W.; Schlegel, H. B.; Scuseria, G. E.; Robb, M. A.; Cheeseman, J. R.; Scalmani, G.; Barone, V.; Petersson, G. A.; Nakatsuji, H., *et al.Gaussian 16*, Revision C.01; Gaussian Inc.: Wallingford CT, 2016.
(47) Stanton, J. F.; Gauss, J.; Cheng, L.; Harding, M. E.; Matthews, D. A.; Szalay, P. G.*CFOUR, Coupled-Cluster Techniques for Computational Chemistry, a Quantum-chemical Program Package*. With contributions from Asthana, A.; Auer, A. A.; Bartlett, R. J.; Benedikt, U.; Berger, C.; Bernholdt, D. E.; Blaschke, S.; Bomble, Y. J.; Burger, S.; Christiansen, O.; Datta, D.; Engel, F.; Faber, R.; Greiner, J.; Heckert, M.; Heun, O.; Hilgenberg, M.; Huber, C.; Jagau, T.-C.; Jonsson, D.; Jusélius, J.; Kirsch, T.; Kitsaras, M.-P.; Klein, K.; Kopper, G. M.; Lauderdale, W. J; Lipparini, F.; Liu, J.; Metzroth, T.; Mück, L. A.; O'Neill, D. P.; Nottoli, T.; Oswald, J.; Price, D. R.; Prochnow, E.; Puzzarini, C.; Ruud, K.; Schiffmann, F.; Schwalbach, W.; Simmons, C.; Stopkowicz, S.; Tajti, A.; Vázquez, J.; Wang, F.; Watts, J. D.; Zhang, C.; Zheng X., and the integral packages MOLECULE (J. Almlöf and P. R. Taylor), PROPS (P. R. Taylor), ABACUS (T. Helgaker, H. J. A. Jensen, P. Jørgensen, and J. Olsen), and ECP routines by A. V. Mitin and C. van Wüllen. For the current version, see http://www.cfour.de.
(48) Pickett, H. The fitting and prediction of vibration-rotation spectra with spin interactions. *J. Mol. Spectrosc.* **1991**, *148*, 371−377.
(49) Kisiel, Z.; Pszczółkowski, L.; Medvedev, I. R.; Winnewisser, M.; De Lucia, F. C.; Herbst, E. Rotational spectrum of *trans-trans* diethyl ether in the ground and three excited vibrational states. *J. Mol. Spectrosc.* **2005**, *233*, 231−243.
(50) Kisiel, Z.; Pszczółkowski, L.; Drouin, B. J.; Brauer, C. S.; Yu, S.; Pearson, J. C.; Medvedev, I. R.; Fortman, S.; Neese, C. Broadband rotational spectroscopy of acrylonitrile: Vibrational energies from perturbations. *J. Mol. Spectrosc.* **2012**, *280*, 134−144.
(51) Winnewisser, G. Millimeter Wave Rotational Spectrum of HSSH and DSSD. II. Anomalous K Doubling Caused by Centrifugal Distortion in DSSD. *Chem. Phys.* **1972**, *56*, 2944−2954.
(52) Typke, V. Centrifugal Distortion Analysis Including P_6-Terms. *J. Mol. Spectrosc.* **1976**, *63*, 170−179.
(53) van Eijck, B. Reformulation of quartic centrifugal distortion Hamiltonian. *J. Mol. Spectrosc.* **1974**, *53*, 246−249.
(54) Watson, J. K. G. Determination of Centrifugal Distortion Coefficients of Asymmetric-Top Molecules. *Chem. Phys.* **1967**, *46*, 1935−1949.
(55) Margulès, L.; Perrin, A.; Demaison, J.; Merke, I.; Willner, H.; Rotger, M.; Boudon, V. Breakdown of the reduction of the rovibrational Hamiltonian: The case of $S^{18}O_2F_2$. *J. Mol. Spectrosc.* **2009**, *256*, 232−237.
(56) Motiyenko, R.; Margulès, L.; Alekseev, E.; Guillemin, J.-C.; Demaison, J. Centrifugal distortion analysis of the rotational spectrum of aziridine: Comparison of different Hamiltonians. *J. Mol. Spectrosc.* **2010**, *264*, 94−99.
(57) Kraitchman, J. Determination of Molecular Structure from Microwave Spectroscopic Data. *Am. J. Phys.* **1953**, *21*, 17−24.
(58) Puzzarini, C.; Bloino, J.; Tasinato, N.; Barone, V. Accuracy and Interpretability: The Devil and the Holy Grail. New Routes across Old Boundaries in Computational Spectroscopy. *Chem. Rev.* **2019**, *119*, 8131−8191.
(59) Watson, J. K. G.*Vibrational Spectra and Structure*; Elsevier: Amsterdam, 1977; Vol. *6*, pp 1−89.
(60) Carpenter, J. H. Convergence of the Reduced Hamiltonian with Centrifugal Distortion in Asymmetric Top Molecules. *J. Mol. Spectrosc.* **1973**, *46*, 348−357.
(61) Helminger, P.; De Lucia, F. C. The ground state rotational spectrum of H_2Se: Weighted microwave-infrared analysis. *J. Mol. Spectrosc.* **1975**, *58*, 375−383.

Recommended by ACS

The Submillimeter Rotational Spectrum of Ethylene Glycol up to 890 GHz and Application to ALMA Band 10 Spectral Line Data of NGC 6334I
Mattia Melosso, Brett A. McGuire, *et al.*
DECEMBER 04, 2019
THE JOURNAL OF PHYSICAL CHEMISTRY A
READ

Why the CC Stretch in HCC Is So Anharmonic
John F. Stanton.
AUGUST 26, 2021
THE JOURNAL OF PHYSICAL CHEMISTRY A
READ

Sulfur Molecules in Space by X-rays: A Computational Study
Goranka Bilalbegović, Susi Lehtola, *et al.*
FEBRUARY 24, 2021
ACS EARTH AND SPACE CHEMISTRY
READ

Evidence of Nonrigidity Effects in the Description of Low-Energy Anisotropic Molecular Collisions of Hydrogen Molecules with Excited Metastable Helium Atoms
Mariusz Pawlak, Piotr Jankowski, *et al.*
MARCH 09, 2020
JOURNAL OF CHEMICAL THEORY AND COMPUTATION
READ

Get More Suggestions >

https://doi.org/10.1021/acs.jpca.2c06038
J. Phys. Chem. A 2022, 126, 8196−8210